

Differential Apoptotic Effects of Novel Quinuclidinone Analogs 8a and 8b in Normal and Lung Cancer Cell Lines

AHMED MALKI^{1,2} and STEPHEN BERGMEIER¹

¹Department of Chemistry and Biochemistry, Ohio University, Athens, OH, 45701, U.S.A.;

²Biochemistry Department, Faculty of Science, Alexandria University, Alexandria, Egypt

Abstract. *Background:* We previously reported novel quinuclidinone analogs that showed both additive and synergistic cytotoxicity in lung cancer cells. We aimed at understanding the mechanism of these analogs and also their cytotoxic effect on normal cells. The effects of these analogs were studied in response to gamma radiation in H1299 human large cell lung carcinoma cells that are null for p53, normal lung epithelial cell line (NL-20) and H1299 cells stably transfected with p53. *Materials and Methods:* The effects of the analogs were investigated by MTT assay, clonogenic survival assay, sphingomylinase activity, Cox-2 activity, ELISA-based apoptotic assay, terminal deoxynucleotidyl transferase dUTP nick end labeling assay, immunofluorescence staining, flow cytometry, real-time reverse transcription polymerase chain reaction and Western blot analysis. *Results:* Our data indicated that 8a and 8b reduced cell proliferation and induced apoptosis in H1299 cells more than H1299-wt p53 cells and NL-20 cells, they also radiosensitize H1299 cells to gamma radiation more than NL-20 cells. 8a and 8b decreased cells in G₂ phase in H1299 cells more than NL-20 cells, which is confirmed by increased expression of cyclin B in H1299 cells, with no significant increase in H1299-wtp53. 8a increased sphingomylinase activity and ceramide level in H1299 more than the rest of cells, it also reduced expression level and activity of COX-2 while it increased caspase-3 activity and induced PARP-1 cleavage. Both derivatives increased expression of p53 in H1299-wt p53 level, while they did not show significant increase in NL-20 cells. Interestingly, these analogs induced apoptosis in H1299 and p53 stably transfected H1299 cells, but they had less effect on normal lung epithelial cells (NL-

20). *Conclusion:* All these results confirm that our quinuclidinone derivatives provoke cytotoxicity in lung cancer cells more than normal cells, which is a feature not present in most chemotherapeutic drugs.

Most cytotoxic agents used to treat cancer act by inducing apoptosis (1, 2). However, a critical flaw in developing and utilizing anticancer drugs is that most also kill normal cells. Hence, it is important to identify compounds that are more potent towards cancer cells than to the normal counterparts. In this work, we report two interesting analogs that have cytotoxic effects on lung cancer cell lines and have less cytotoxic effects on normal lung epithelial cells.

Previously, our lab reported novel quinuclidinone analogs that induce cytotoxicity in a human non-small lung carcinoma cell line (H1299) null for p53 (3). However, the mechanisms by which these analogs induce cytotoxicity were poorly understood. Here we examine the nature of the growth inhibition in H1299 cells, H1299-wt p53 cells, NL-20 cells and the key players involved. The tumor suppressor gene, p53, is a key component of a cellular emergency response system which induces cell growth arrest or apoptosis (4). Inactivation and mutations of p53 in cancer may be responsible for accelerated cell growth and resistance to therapeutic drugs (5, 6). We previously identified methylxanthine derivatives that differentially radiosensitize lung cancer cells depending upon p53 status (7). The signaling cascade induced by p53 is likely to be complex and may differ depending on the type of tissue examined (9-11).

Apoptosis is a regulated biochemical process that balances cell survival and death, maintaining normal tissue homeostasis (12). In the molecular event of apoptosis, it has been thought that mainly kinases and caspases are central in mediating and transducing signals, but emerging reports showed that lipid molecules also play a crucial role. Different kinds of lipids reside in cell membranes, and they could be released and transduce a signal from extracellular stimuli (13-15). In fact, during apoptosis the concomitant ceramide formation from sphingomyelin hydrolysis brings about changes in membrane topology, which is the hallmark of

Correspondence to: Ahmed Malki, Ph.D., Biochemistry Department, Faculty of Science, Alexandria University, Moharam, Beck, PO BOX 25115, Alexandria, Egypt. Tel: +20 20122267456, Fax: +2033900042, e-mail: amalky@yahoo.com

Key Words: Anticancer agents, sphingomylinase, Cox-2, caspase-3, apoptosis, p53, cell cycle.

apoptosis (16). Ceramide is well established as a bioactive molecule, implicated in processes such as the cellular response to stress, cell growth and apoptosis. Additionally, sphingomyelin hydrolysis by sphingomyelinases (SMases) has emerged as a key pathway of stress-induced ceramide generation (17, 18). Recent studies have highlighted the relevance of cyclooxygenase 2 (COX-2) in human carcinogenesis. Increased levels of COX-2 have been reported in numerous tumors, including head and neck squamous cell cancer, as well as colorectal, breast, lung, skin stomach, liver, and other types (19-23). Selective inhibition of COX-2 is considered a novel therapy in both the chemoprevention and treatment of solid tumors. Experimental animal data indicate that COX-2 gene may be associated with carcinogenesis of several types of human malignancies (24, 25).

Caspases are cysteine proteases, which are either described as initiator caspases 2, 8, 9, 10 and 12 or as effector caspases 3, 6 and 7. Caspase-8 and -9 are the two main initiator caspases that are activated through the death receptor and the mitochondrial pathway, respectively. Caspase-3 activation marks the key process of nuclear apoptosis, where it cleaves important apoptotic inducers, such as DNA fragmentation factor 45 (DFF45), poly-(ADP-ribose) polymerase (PARP), acinus and lamin (26, 27).

We have previously synthesized novel quinonucleodione analogs and reported preliminary evidence of their cytotoxic effect in lung cancer cell lines (Figure 1). Our novel derivatives (8a and 8b) induced apoptosis in lung cancer cells null for *p53* more than normal lung epithelial cells (NL-20) and *p53* stably transfected H1299 by radiosensitizing H1299 cells to gamma radiation, reducing cells in G₂/M phase, increasing caspase-3 activity and reducing COX-2 activity. 8a increased sphingomyelinase activity and ceramide levels in *p53* null cells, while 8b increased its activity in transfected cells. *p53* was overexpressed by both analogs in both normal lung epithelial cells and *p53*-stably transfected cells, while BAX expression increased in *p53* null cells than *p53* stably transfected cells. The difference in activity between normal and non-small cell lung carcinoma (NSCLC) cells may be responsible for their diverse effects. Investigational studies on more cancer cell lines and *in vivo* studies are in progress in order to give more information about the mechanism of action of these unique analogs.

Materials and Methods

Cell culture and drug treatment. H1299 cells that have a deletion of the *p53* gene were derived from a human large cell lung carcinoma (provided by Jack Roth, M.D. Anderson Cancer Center, Texas, USA). Cells were maintained in Dulbecco's modified essential media (DMEM) (Gibco, Carlsbad, CA, USA) supplemented with 10% fetal bovine serum (FBS), 100 U/ml penicillin, and 100 µg/ml streptomycin at 37°C in a 5% CO₂ atmosphere (Gibco). NL-20, a normal lung epithelial cell line (ATCC, Manassas, VA, USA), was

maintained in DMEM/F-12 media (Gibco) supplemented with 10% FBS, 100 U/ml penicillin, 100 µg/ml streptomycin, insulin (1.2 g/L), transferrin (0.001 mg/ml), epidermal growth factor (EGF) (20 ng/µL) and hydrocortisone (500 ng/ml) at 37°C in a 5% CO₂ atmosphere. H1299 cells were stably transfected with wild-type *p53* and maintained in supplemented DMEM described above. Cells were transfected using Lipofectamine (Invitrogen, CA, USA) and stable transformants were selected with G418 (300 mg/L). All selected quinuclidinone analogs were prepared at a concentration of 100 µM and dissolved in suitable media.

Methyl tetrazolium (MTT) bromide mitochondrial activity assay. Cell viability was measured by the MTT bromide mitochondrial activity assay (ATCC). Briefly, 4000-5000 cells/well in 100 µL of medium were seeded in a 96-well plate for 24 h prior to drug treatment. The media was then changed to media with analogs (100 µM) and cells were treated with gamma radiation (4 Gy). After 24 hours, 10 µL of 5 mg/mL MTT reagent was added to each well cells were and incubated for 4 h. After incubation, 100 µL of detergent reagent was added to each well to dissolve the formazan crystals. The absorbance was determined at a wavelength of 570 nm. Cells treated only with irradiation were used as controls. Each assay was performed in triplicate and standard deviation determined.

Clonogenic survival assay. Cell survival following gamma radiation was measured by clonogenic assays in monolayer in 10 cm plates. Cells were plated in triplicate and were grown for 2 days to approximately 70% confluency. Quinuclidinone analogs were dissolved in culture media at a final concentration of 100 µM and added to the plated cells 30 min prior to irradiation. Cells were irradiated with different doses of gamma radiation, ranging from 2.5-10 Gy, from a ¹³⁷Cs source (J. L. Shepherd and Associates, CA, USA). After 24 h, the media containing the analogs was removed and replaced with fresh media without the derivatives. The cells were grown for 14 days to monitor colony formation. Colonies of at least 50 cells were scored as clonogenic survivors. The surviving fraction was determined by the proportions of seeded cells that formed colonies after drug and radiation treatment relative to the control cells, which were irradiated with gamma radiation without prior drug treatment. Each data point was derived from the results of 3 independent experiments and expressed as mean±standard deviation.

Enzyme-linked immunosorbent apoptosis assay (ELISA). Cells were seeded at a density of 2×10⁴/well in a 96-well plate and incubated for 24 hours. Media was changed to media containing the different analogs (100 µM) 30 min before irradiation. Cells were then incubated for 24 hours. ELISA was performed using Cell Death Detection ELISAPLUS kit (Roche-Applied Science, IN, USA) that measures histone release from fragmented DNA in apoptosing cells. Briefly, cells were lysed with 200-µL lysis buffer for 30 min at room temperature. The lysate was centrifuged at 200 ×g for 10 min. 150 µL of supernatant was collected, of which 20 µL was incubated with anti-histone biotin and anti-DNA peroxidase at room temperature for 2 h. After washing with incubation buffer three times, 100 µL of substrate solution (2,2'-azino-di(3-ethylbenzthiazolin-sulphuric acid) was added to each well and incubated for 15-20 min at room temperature. The absorbance was measured using an ELISA reader (Spectra Max Plus; Molecular Devices, Carlsbad, CA, USA) at 405 nm. The control group were cells treated with either UV or gamma radiation. Each assay was carried out in triplicate and standard deviation determined.

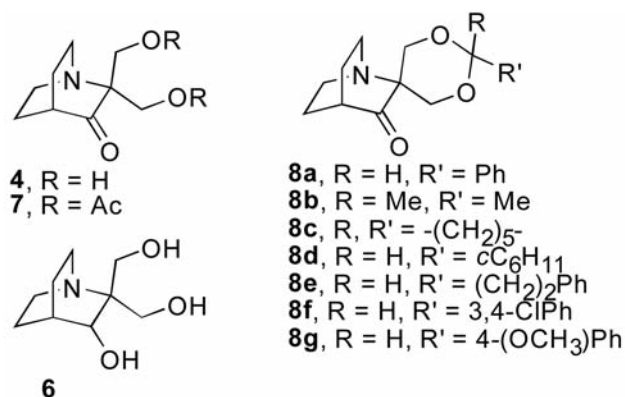


Figure 1. Structure of selected quinuclidinone analogs.

TUNEL and DAPI staining. For *in situ* detection of apoptotic cells, terminal deoxynucleotidyl transferase dUTP nick end labeling (TUNEL) assay was performed using DeadEnd™ fluorimetric tunnel system (Promega, Madison, WI, USA). Cells were cultured on 4-chamber slides (VWR, Radnor, PA, USA) at a density of 2×10^4 cells/ chamber. After treatment with 100 μM of the derivatives, cells were washed with phosphate-buffered saline (PBS) and fixed by incubation in 4% paraformaldehyde (PFA) for 20 min at 4°C. The fixed cells were then incubated with digoxigenin-conjugated dUTP in terminal deoxynucleotide transferase recombinant (rTdT)-catalyzed reaction and nucleotide mixture for 60 min at 37°C in a humidified atmosphere and then immersed in stop/wash buffer for 15 min at room temperature. Cells were then washed with PBS to remove unincorporated fluorescein-12-dUTP. After washing with PBS, cells were incubated in 1 $\mu\text{g}/\text{ml}$ DAPI (4',6-diamidino-2-phenylindole) solution for 15 min in dark (data not shown). Cells were observed with fluorescence microscopy (RT slider Spot, Diagnostic Instruments, Inc) and photographed at $\times 100$ magnification.

Flow cytometric analysis. Cells were seeded at a density of $3\text{-}5 \times 10^5/10$ cm plate and incubated for 24 h before radiation. Media was changed to media containing the different analogs (100 μM), 30 min before irradiation. Cells were exposed to 4 Gy gamma radiation. 24 h after drug and radiation treatment, cells were harvested by trypsinization. The cells were washed with PBS and fixed with ice-cold 70% ethanol while vortexing. Finally, the cells were washed and resuspended in PBS containing 5 $\mu\text{g}/\text{mL}$ RNase A (Sigma, St. Louis, MO, USA) and 50 $\mu\text{g}/\text{mL}$ propidium iodide (Sigma) for analysis. Cell cycle analysis was performed using FACScan Flow Cytometer (Becton Dickson, Bohemia, NY, USA) according to the manufacturer's protocol. Windows multiple document interfaces (WinMDI, Bohemia, NY, USA) software was used to calculate the cell-cycle phase distribution from the resultant DNA histogram, and expressed as a percentage of cells in the G_0/G_1 and G_2/M phases. The apoptotic cells were determined on the DNA histogram as a subdiploid peak.

Sphingomylinase assay. Sphingomylinase activity was determined *in vitro* by Amplex Red sphingomylinase assay (Molecular probes, Carlsbad, CA, USA) in a 96-well microplate reader according to

manufacturer's protocol. Briefly, 4,000-5,000 cells/well in 100 μL of medium were seeded in a 96-well plate for 24 h prior to drug treatment. The media was then changed to media with analogs (100 μM). Samples were diluted with reaction buffer and pipetted into a 96-well microplate. 100 μL of 100 μM (Amplex Red reagent; Molecular Probes, Carlsbad, CA, USA) containing 2 U/ml horseradish peroxidase (HRP), 0.2 U/ml choline oxidase, 8 U/ml alkaline phosphatase and 0.5 mM sphingomyline working solution was added to each sample and incubated for 30 min, protected from light. Fluorescence was measured in a fluorescence microplate reader (Spectra Max Plus;) using excitation range of 530-560 and emission detection at 590 nm.

Ceramide measurement. Ceramide was quantified by the diacylglycerol (DAG) kinase assay. Briefly, cells were extracted with methanol:chloroform:1 N HCl (100:100:1, v/v/v). The lipids in the organic phase were dried under vacuum, resuspended in 100 μl of reaction mixture containing $[\gamma\text{-}^{32}\text{P}]\text{ATP}$, and incubated at room temperature for 1 h. The reactions were terminated by extraction of lipids with 1 ml of methanol-chloroform-1 N HCl, 170 μl of buffered saline solution, and 30 μl of 0.1 M ethylenediaminetetra-acetic acid (EDTA). The lower organic phase was dried under vacuum, and the lipids were resolved by thin-layer chromatography on silica gel 60 plates (Whatman, Piscataway, NJ, USA) using a solvent of chloroform-methanol-acetic acid (76:18:6, v/v/v). ^{32}P -labeled ceramide-1-phosphate was detected by a phosphoscreen and analyzed by a phosphorimager machine (Lab X, Midland, ON, Canada). All treatments for ceramide analysis were done in duplicate; each experiment was repeated three times.

COX-2 assay. COX-2 activity was determined according to manufacturer's control (Assay Designs, Ann Arbor, MI, USA). Briefly, 10^7 cells were lysed by sonicating cells in TNE (Tris-NaCl-EDTA buffer containing 10 mM Tris, pH 8, 0.15 M NaCl, 1% NP-40, 1 mM EDTA). The supernatant was collected and after 5 min centrifugation at 15,000 rpm and assayed immediately. A standard curve was constructed using different concentrations of human COX-2 according to manufacturer's protocol, from which the concentrations of samples were determined. One hundred microliters of primary antibody was added to each sample and incubated at 4°C for 30 min. Then the wells were washed 2-3 min. One hundred microliters of substrate was added and incubated in dark for 30 min and reaction was stopped by adding 100 μL 1 N sulfuric acid. Optical density was determined at 450 nm against blank (Spectra Max Plus; Molecular Devices).

Caspase-3 activity. Caspase-3 activity was assayed according to manufacturer's protocol (Assay Designs). Briefly, 5×10^6 cells were lysed in 100 μL lysis buffer containing 10 mM HEPES (4-(2-hydroxyethyl)-1-piperazineethanesulfonic acid), pH 7.4, 2 mM EDTA, 0.1% 3-[(3-cholamidopropyl)dimethylammonio]-1-propanesulfonate (CHAPS), 5 mM, 350 $\mu\text{g}/\text{ml}$ phenylmethylsulfonyl fluoride (PMSF) and 5 mM dithiothreitol (DTT). Cell were homogenized by three cycles of freezing and thawing and then centrifuged to remove the cellular debris. Each sample was then incubated in buffer containing 10 mM HEPES, pH 7.4, 2 mM EDTA, 0.1% CHAPS, 5 mM EDTA supplemented with Ac-DEVD-AFC (acetyl-Asp-Glu-Val-Asp-7-amino-4-trifluoromethylcoumarin) for 1 hour at room temperature and then reaction was stopped with 1 N HCl. OD_{405} was measured using a spectrophotometer (Spectra Max Plus; Molecular Devices).

Transfection of p53. H1299 cells were transfected with pCMV-p53 (human) plasmid using Lipofectamine (Gibco) as recommended according to manufacturer's protocol. Briefly, solution A and solution B (Lipofectin reagents; Invitrogen) were mixed and incubated for 20 minutes. The Lipofectin-DNA solution was added to cells, plated at $1 \times 10^5/10$ cm plates and incubated for 6 hours at 37°C in a CO₂ incubator. The media was aspirated and changed to normal media. G418 (300) mg/L (Gibco) was added to the culture to select from transfected cells. After 3 weeks, single independent cell clones were isolated and each clone was plated independently.

Western blot analysis. The expression of p53, COX-2, cyclin B and PARP-1 was tested by Western blotting analysis using p53 stably transfected cells and normal lung epithelial cells. The samples were normalized and the loading dye (50 mM Tris-Cl pH 6.8, 100 mM β -mercaptoethanol, 2% SDS, 0.1% bromophenol blue, 10% glycerol) was added. The samples were heated at 95°C for 5 min and the proteins separated on sodium dodecyl sulfate polyacrylamide gel electrophoresis (SDS-PAGE). The proteins were then transferred to polyvinylidene difluoride (PVDF) transfer membrane (Millipore Corporation, MA, USA) using a semi-dry transfer apparatus (OWL; Biocompare, San Francisco, CA, USA). The membrane was blocked with 5% non-fat milk in PBS containing 0.25% tween-20 (Sigma-Aldrich, MO, USA) (PBS-T) at room temperature (RT) for 1 h and then incubated with the appropriate primary antibodies (Bp-53 monoclonal mouse antibody; Santa Cruz Biotechnology, Santa Cruz, CA, USA) at a 1:500 dilution in 5% milk PBS-T overnight at 4°C. The membrane was washed quickly three times and then two 5 min wash and incubated with the appropriate secondary antibody conjugated to HRP (goat anti mouse antibody, Santa Cruz Biotechnology) at a 1:20,000 dilution in 5% milk PBS-T for 1 h at RT. The membrane was washed in PBS-T, three quick washes and three 15 min washes to remove unbound antibodies and proteins were detected by autoradiography using the ECL Advanced Western Blotting Detection Kit (Amersham Biosciences, NJ, USA).

Real-time quantitative RT-PCR. H1299 cells and p53 stably transfected cells were cultured in 5% CS and 1% penicillin streptomycin-containing DMEM to 60% confluency and then the cells were switched to new culture media supplemented with 100 μ M of derivatives. After 48 h, RNA was extracted using RNeasy total RNA extraction kit (Qiagen, Inc., Valencia, CA, USA) according to the manufacturer's protocol. The quality of RNA was verified using 12% formaldehyde agarose gel electrophoresis and the concentration of the total RNA extracted was measured using spectrophotometer at 260 nm. 3 μ g of the total extracted RNA was subjected to RT-PCR and cDNA was synthesized using the Biorad iScript™ Select cDNA Synthesis kit (Biorad, Hercules, CA, USA) containing random and oligo DT primer mix. The cDNA produced was used to specifically quantify the transcript of interest using RT² PCR. The primers for the house-keeping gene GAPDH were forward, 5'-AGCCACATCGCTCAGACAC; reverse, GCCCAATACGACCAAA TCC. BAX forward primer: GCAGGGAGGA TGGCTGGG GAG and BAX reverse primer: TCCAGACAAGCAAGCAGCGCTTCA GC. The SyBr green dye intercalates with the double-stranded cDNA being formed during PCR, allowing an easy quantification of cDNA to indirectly quantify the original RNA transcripts present. Thermal cycling conditions were designed as follows: RNA retro-transcription at 48°C for 30 min

followed by an initial denaturation at 95°C for 10 min and 40 cycles of 95°C for 15 s and 60°C for 1 min. The relative quantification of gene expression was performed using the comparative C_T method (Ct). Each evaluation was performed in triplicate in three independent experiments.

Statistical analysis. All data were analyzed by Student *t*-test and expressed as mean \pm standard deviation. A *p*-value of less than 0.05 was considered statistically significant. All of the experiments were carried out in triplicate.

Results

Effect of quinuclidinone analogs on cell viability. Our initial screening used MTT assay using 100 μ M concentration of quinuclidinone analogs in H1299 cells, NL-20 cells and p53 stably transfected H1299 cells (Figure 2 A, B and C). In H1299 cells, both the benzylidine analog (8a) and acetonide derivative (8b) showed significant decrease in cell viability compared with all the other analogs. Their effect was more efficient and synergistic when combined with gamma radiation (Figure 2A). In p53-stably transfected cells the pattern of cell viability was changed, as with many analogs, including the lead compound 4, showing a more efficient decrease in cell viability (Figure 2B). However, 8a and 8b still are the most potent analogs. Interestingly, in NL-20 cells, 8a and 8b had less cytotoxic effect on cell viability, while other analogs (8c, 8d, 8e) were more potent and cytotoxic to normal (Figure 2C). Cytotoxicity was determined in the presence of 100 μ M cisplatin as a control chemotherapeutic drug (Figure 2D).

Apoptotic response by quinuclidinone analogs. Apoptosis was examined in H1299, NL-20 and p53 stably transfected H1299 cells after treating them with 100 μ M of the selected analogs by ELISA, in order to detect histone release. In both H1299 cells and p53 stably transfected cells, 8a and 8b increased induction of apoptosis compared to all other analogs. However, their effect was slightly lower in transfected cells. Interestingly, in NL-20 cells, 8a and 8b were the analogs least able to induce apoptosis, whereas 6c, 8c, 8d and 8e greatly increased apoptosis (Figure 3A).

TUNEL assay. TUNEL assays were performed in order to ascertain induction of apoptosis by 8a and 8b H1299 and p53-stably transfected cells. In H1299 cells, the assay revealed the presence of nuclear condensation and TUNEL-positive cells after treating cells with 100 μ M of 8a and 8b (Figure 3B). Fewer TUNEL-positive cells were found after treating p53 stably transfected H1299 cells with the same derivatives (Figure 3B).

Effect of quinuclidinone analogs on cell survival after radiation. Cell survival was measured by clonogenic assays after drug treatment and gamma radiations. 8a and 8b

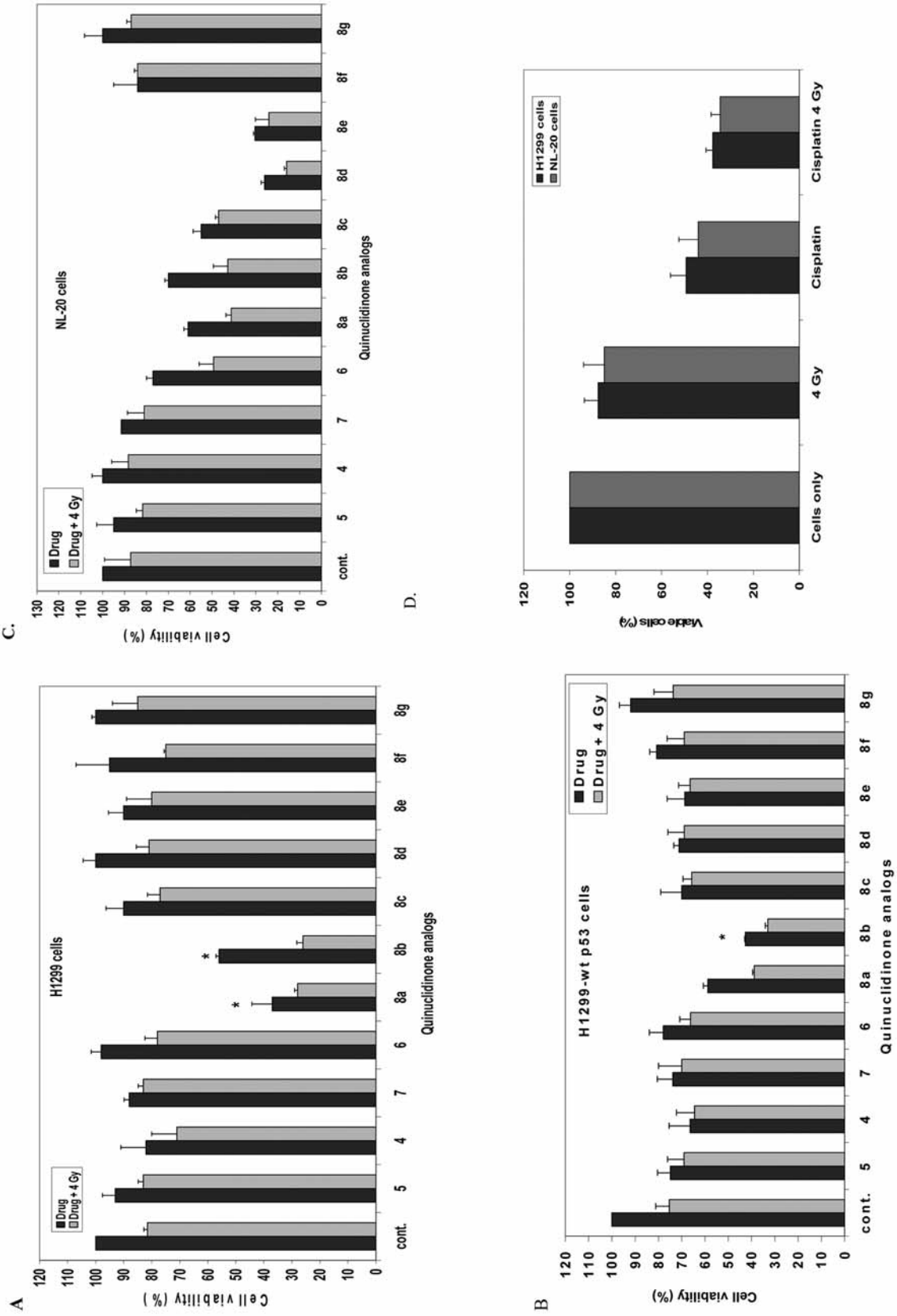


Figure 2. Effect of quinuclidinone derivatives on cell viability of H1299 cells (A), p53 stably transfected cells (B) and NL-20 cells (C) in the presence and absence of gamma radiation. Cisplatin was used as control to monitor cytotoxicity towards normal and lung cancer cells (D). Each data point is an average of three independent experiments and expressed as the mean ± SD. All experiments were carried out with 100 μM of each derivative.

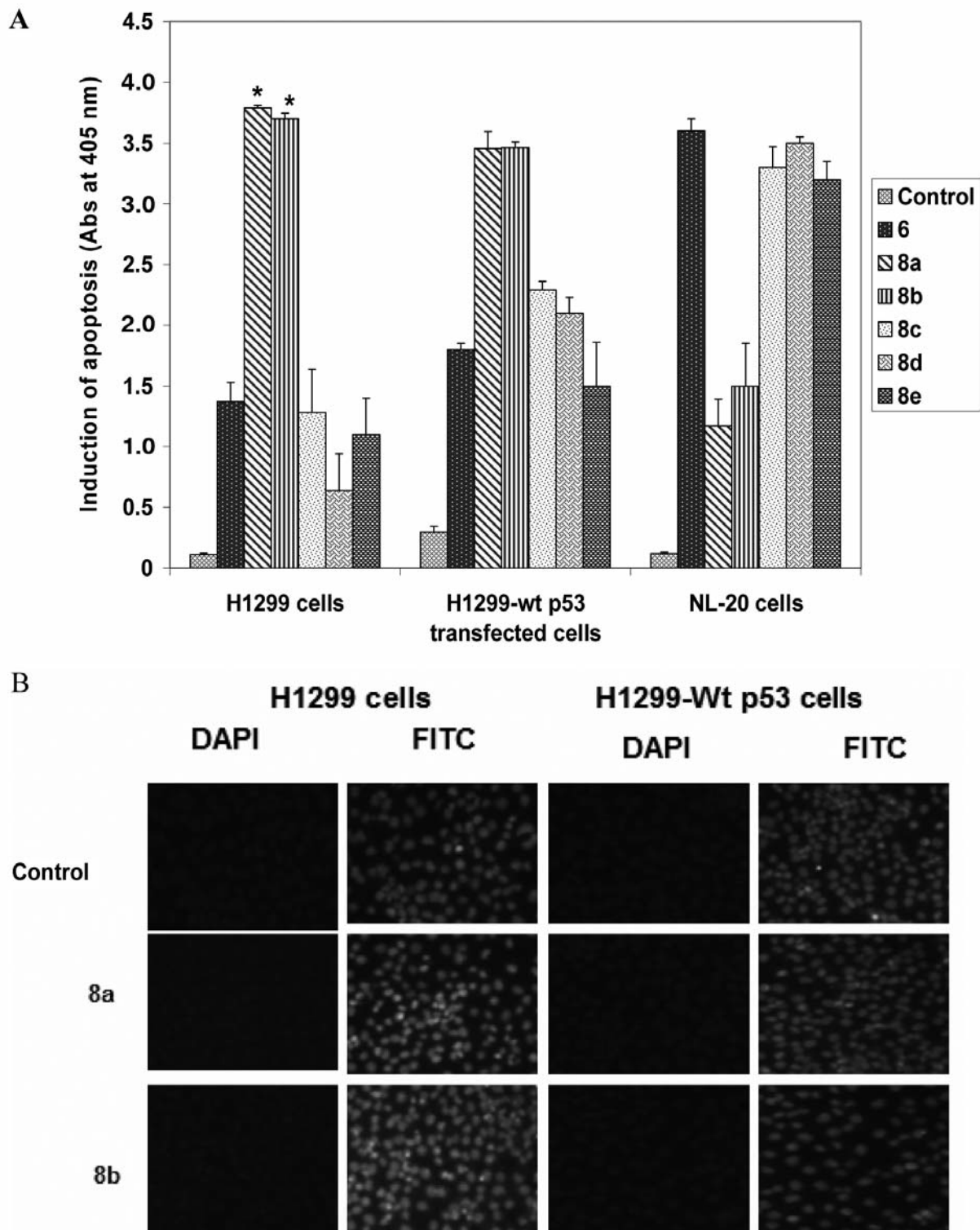


Figure 3. Induction of apoptosis in H1299 cells, NL-20 cells and H1299-wt transfected cells with 100 μ M analogs and 24 h duration interval. Each data point is the mean of three independent experiments and expressed as mean \pm SD. Induction of apoptosis is represented by absorbance at 405 nm. Characterization of induced cell death in H1299 (A) cells and p53 stably transfected cells (B). Cells were treated with DAPI and stained via TUNEL assay. Cells were treated with 100 μ M of 8a and b and compared to control (non-treated cells). DAPI was used to stain the nuclei. FITC: Fluorescein-12 dUTP labeled DNA.

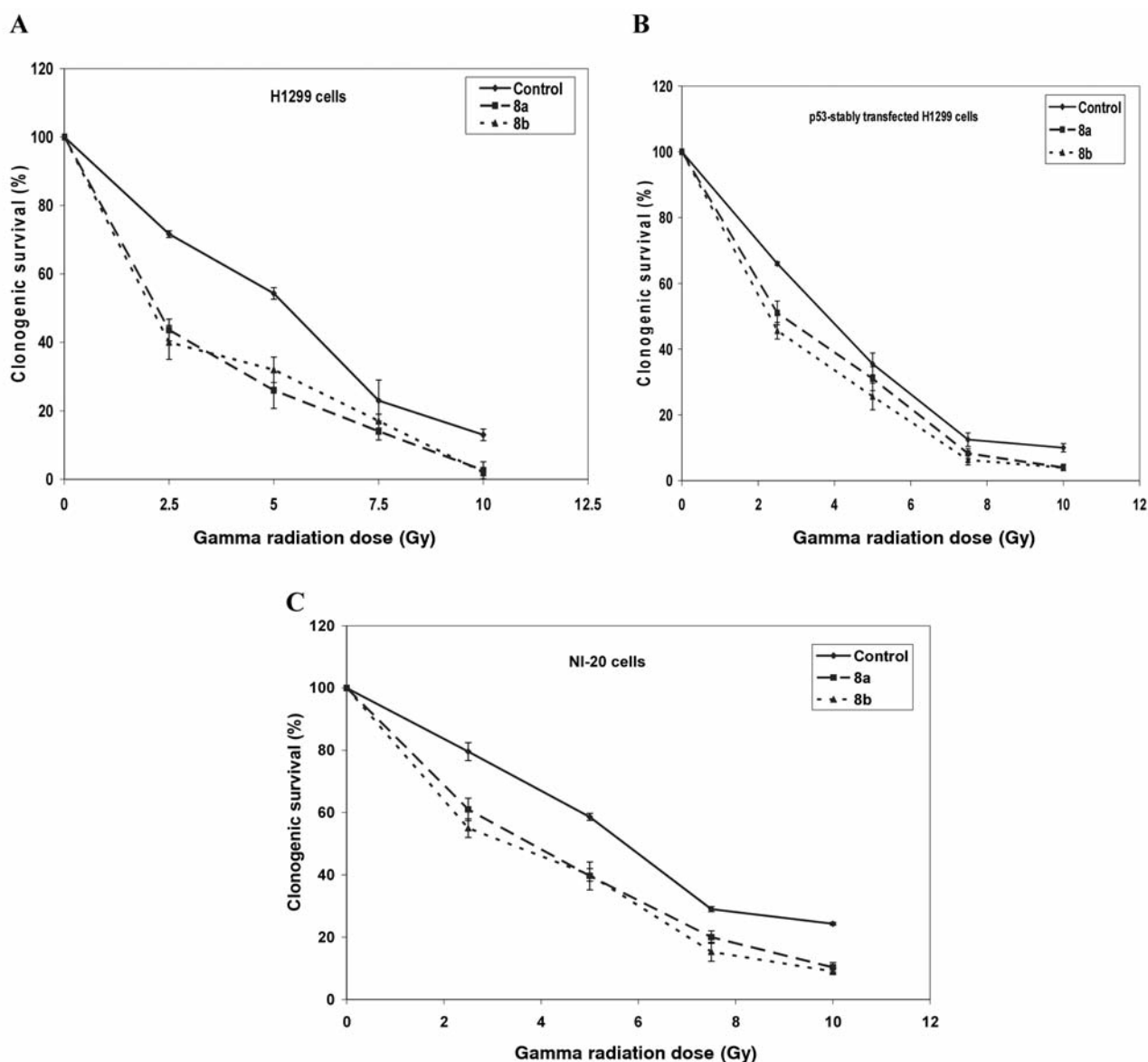


Figure 4. Effect of different doses of gamma radiation on clonogenic survival in H1299 cells (A), NL-20 cells (B) and H1299-wt p53 transfected cells (C) with (100 μ M) of different quinuclidinone derivatives. Each data point is an average of three independent experiments and expressed as mean \pm SD.

decreased cell proliferation synergistically in the presence of different doses of gamma radiation (2.5-10 Gy) in H1299 cells, p53 -stably transfected cells and normal lung epithelial cells (Figure 4A, B, C) in a dose-dependent manner. The effects of 100 μ M analogs were compared to the control group that consisted of cells treated only with irradiation. Although 8a and 8b are non-significantly different, they are significantly different from the control group. 8a and 8b greatly decreased clonogenic survival in H1299 more than corresponding p53 stably transfected cells (Figure 4A, B). 8a and 8b had less effect on clonogenic survival in NL-20 cells

than lung cancer cell lines (Figure 4C). In all tested cell lines, the percentage of clonogenic survival at higher doses of gamma radiation (7.5 and 10 Gy) was greatly reduced to less than 10%.

Impact of quinuclidinone analogs on cell cycle checkpoints using flow cytometry. Flow cytometry was used to examine the effects of the derivatives on cell cycle checkpoints as well as cell proliferation or apoptosis. The percentage of cells in G₁, S, G₂, and apoptosis were determined after treating cells with different analogs (100 μ M) (Figure 5A, B,

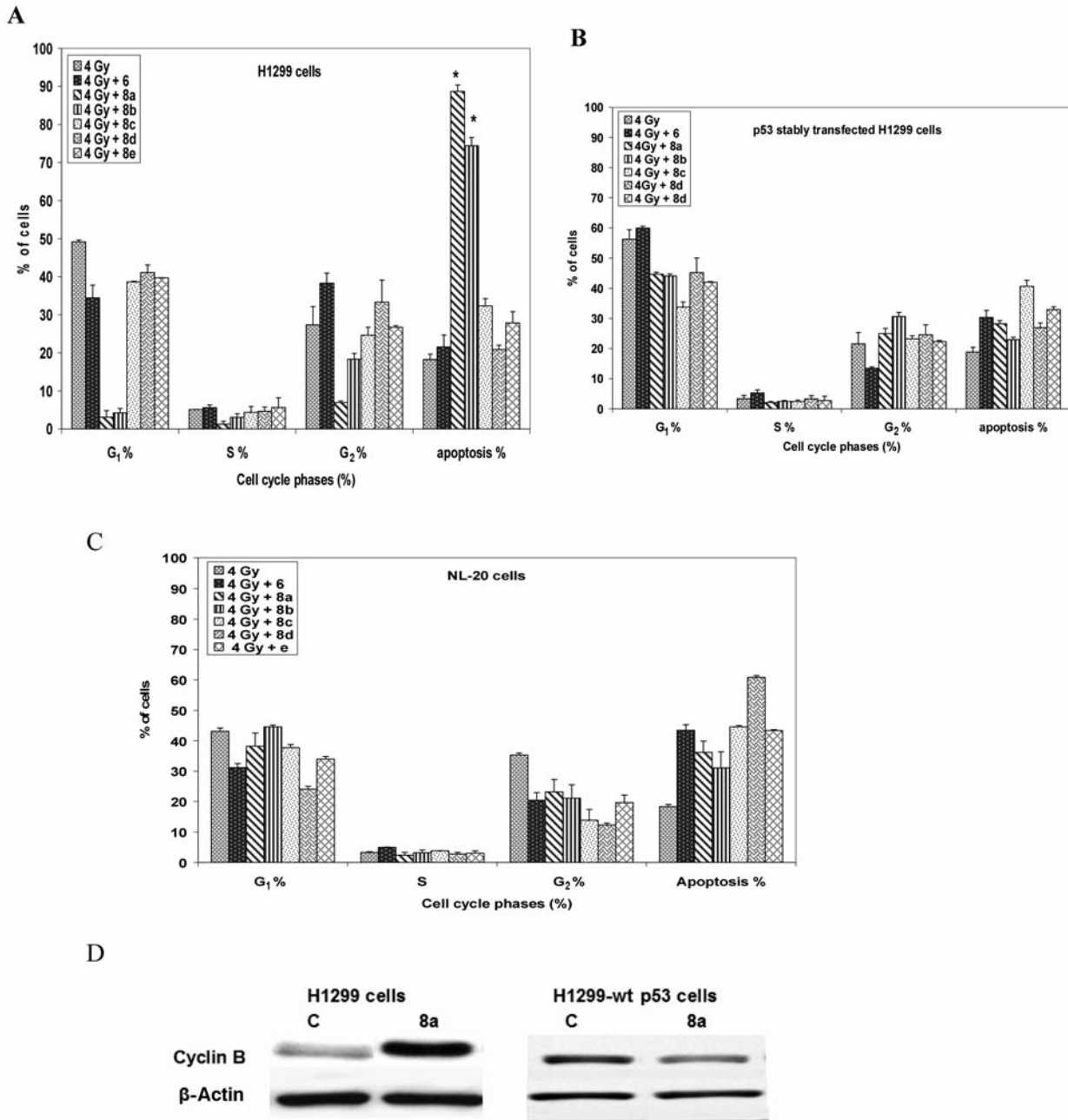


Figure 5. Impact of quinuclidinone derivatives on cell cycle phases in H1299 (A) cells and H1299-wtp53 transfected cells (B) and , NL-20 cells (C) at 4 Gy of gamma radiation and 24 h duration interval. Each data point is the mean of three independent experiments and expressed as the mean \pm SD. Expression of cyclin B was determined by Western blot analysis using β -actin as control (D).

and C). H1299 cells that were irradiated and harvested 24 h post irradiation showed an increase in the percentage of G₁ cells compared to G₂ (49% versus 27%, respectively) ($p < 0.05$), which indicates that cells were arrested in G₁ phase. However, both 8a and 8b significantly reduced the number of cells arrested in G₁ (3% and 4%, respectively) compared to irradiated cells (49%), ($p < 0.05$) and they also

significantly reduced the number of cells in G₁ (7% and 18% respectively) compared to the irradiated group (27%) ($p < 0.05$). They also significantly increased the percentage of apoptosis after radiation in H1299 cells to 89% and 74% respectively ($p < 0.05$) compared to the irradiated group (18%) (Figure 5A). In p53 stably transfected cells, 8a and 8b slightly decreased the number of cells in G₁ phase, increased

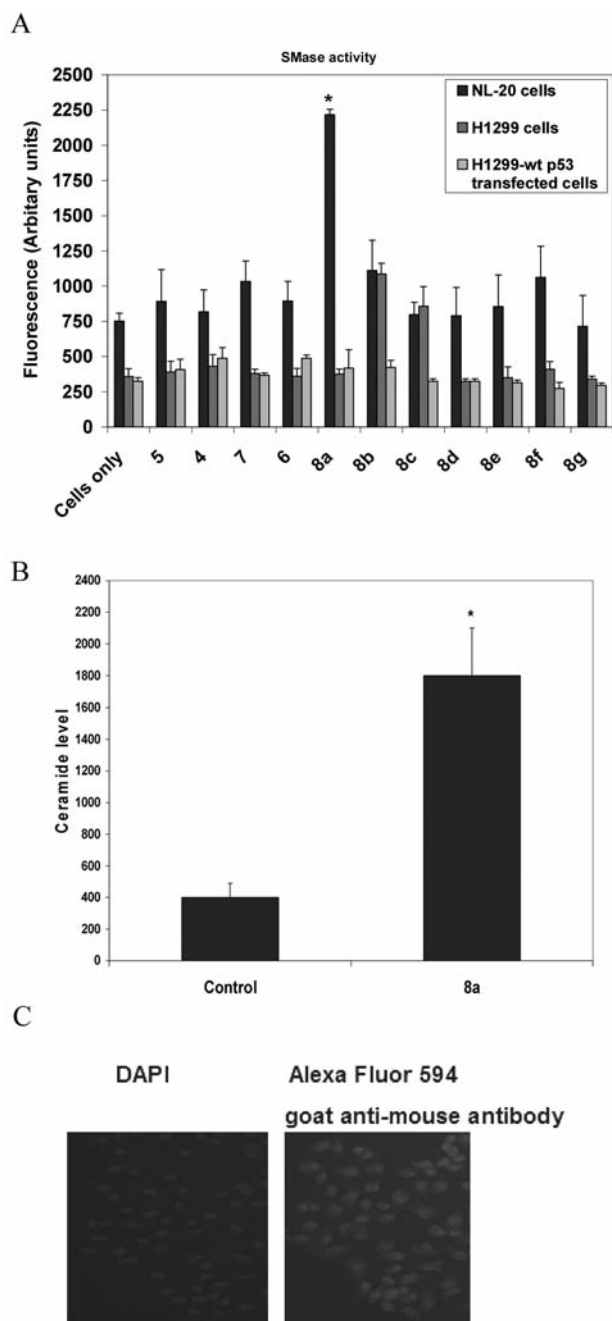


Figure 6. Impact of 8a and 8b on sphingomyelinase activity in H1299 cells, p53 stably transfected cells and NL-20 cells in the presence and absence of gamma radiation (A). Each data point is the average of three independent experiments and expressed as the mean \pm SD. All experiments were carried out with 100 μ M of each derivative. Ceramide was quantified by the diacylglycerol (DAG) kinase assay (B) and expressed as the mean \pm SD and Detection of ceramide by IHC was performed with anti-ceramide MAb (C).

the number of cells in G₂ phase to 25% and 31% compared to the irradiated control group 22%, and induced apoptosis to 28% and 23% compared to the irradiated group, 19%

(Figure 5B). In NL-20 cells, 8a and 8ab were the analogs least able to induce apoptosis (36% and 31%, respectively). They abrogated the G₂/M checkpoint and directed cells to apoptosis without significant effect on the G₁ checkpoint (Figure 5C). The expression level of cyclin B was significantly increased upon 8a treatment in H1299 cells, while there was significant change in H1299-wt p53 cells (Figure 5 D).

Sphingoylinase assay. SMases represent central elements of the so-called sphingomyelin/ceramide signaling pathway, which play an important role in the induction of apoptosis. We tested SMases activity for all the analogs (100 μ M) in H1299 cells, p53- stably transfected H1299 cells, and normal lung epithelial cells (Figure 6A). In H1299, only 8a significantly increased SMases activity, to almost double the activity of all the other analogs, including the control group. In p53 stably transfected cells, only 8b and 8c increased SMases activity compared to all the other analogs. In NL-20 cells, none of the derivatives had an effect on SMases activity. 8a was capable of inducing significant increases in ceramide levels in exposed cells compared with non-treated cells (Figure 6 B).

COX-2 activity. COX-2 is an inducible enzyme expressed in response to cytokines, growth factors, and it is also overexpressed in non-small cell lung carcinoma (NSCLC). Our data showed that COX-2 is overexpressed in H1299 cells compared to p53 stably and NL-20 cells. There was a significant reduction of COX-2 activity in H1299 cells by 8b followed by 8a (Figure 7A). Similar results were found in p53 stably transfected cells and less reduction of COX-2 activity by 8a and 8b was found in NL-20 cells. These results indicate that our derivatives might serve as potential COX-2 inhibitors. Both 8a and 8b reduced COX-2 expression level in H1299 cells by Western blot analysis (Figure 7B).

Caspase-3 activity and PARP-1 cleavage. As caspase-3 appears to be the predominant caspase involved in p53-induced cell death, we determined the effect of the most potent analogs on caspase-3 activity. There was a slight increase in caspase-3 activity after irradiating cells with 4 Gy gamma radiation, while there was a significant increase in its activity after treating cells with 8a and 8b in combination with gamma radiation compared to the control and the irradiated only group. In p53 stably transfected cells, there was a slight and non-significant increase in caspase-3 activity, although there was an increase in its activity after irradiation only (Figure 7C). The increase in caspase-3 activity in H1299 cells was further confirmed by determining PARP-1 cleavage. The results seen in Figure 7D indicate that 8a increased expression of PARP-1 (80 kDa) in H1299 cells.

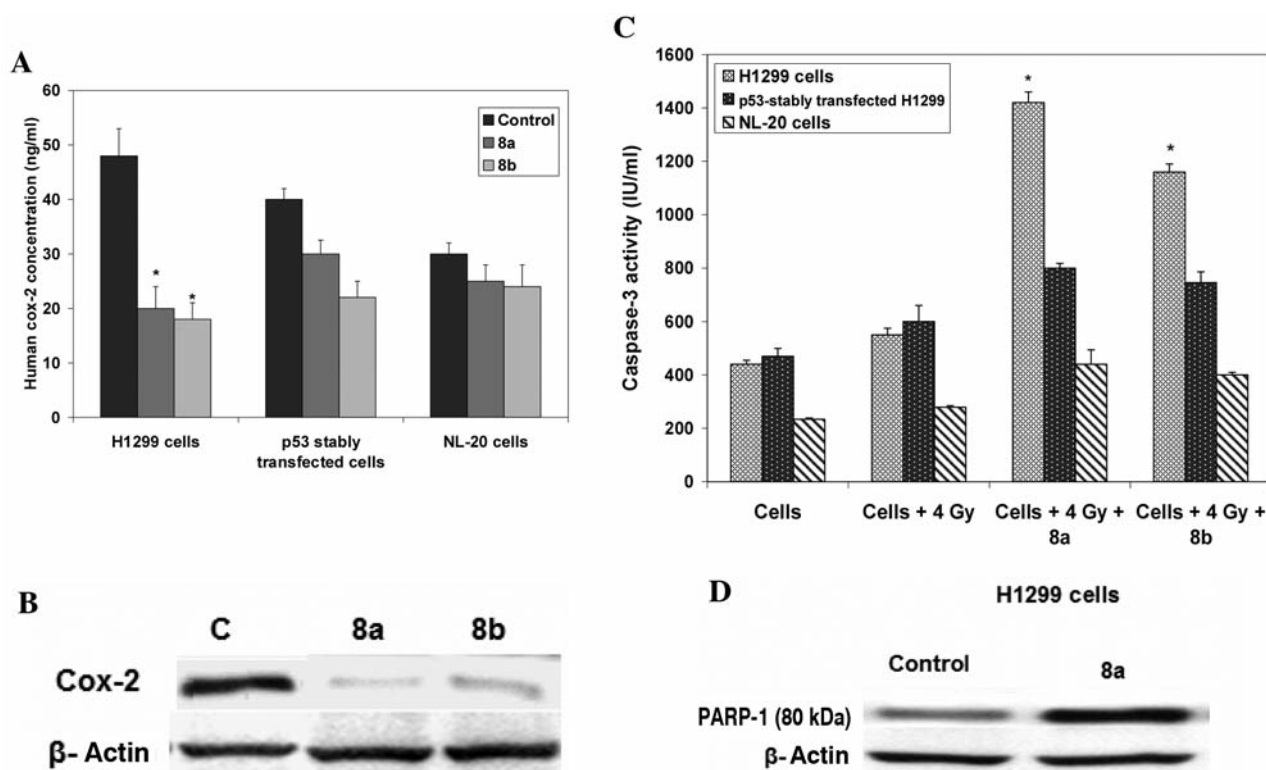


Figure 7. Impact of quinuclidinone derivatives COX-2 activity, Caspase -3 and Parp1 cleavage. was determined in H1299 cells, p53 stably transfected cells and NL-20 cells in the presence of 100 μ M 8a and 8b. Effect of quinuclidinone derivatives on COX-2 activity (A, B), caspase-3 activity (as indicated by (DEVD-pNA) cleavage) (C) and PARP-1 cleavage (D) in H1299 cells, p53 stably transfected cells and NL-20 cells in the presence of 100 μ M 8a and 8b. Each data point is an average of three independent experiments and expressed as the mean \pm SD.

p53 protein expression. H1299 cells were stably transfected with *p53* and expression of *p53* was determined (Figure 8A and Figure 8B). In both NL-20 and *p53* stably transfected cells, *p53* was overexpressed after treating cells with 100 μ M 8a and 8b compared to the irradiated group. However, there was significant expression of *p53* in *p53* stably transfected cells compared to NL-20 cells.

BAX expression and immunohistochemical staining. BAX, a primary target of *p53*, induces cell death through disruption of mitochondrial permeability and subsequent release of cytochrome c. We wanted to see if BAX is a downstream target of *p53* in a *p53*-dependent or a *p53* independent apoptotic pathway. The data showed that 8a and 8b increased BAX protein level in comparison to the control group alone, in H1299 cells more than H1299-wt *p53* (Figure 9A). Immunohistochemistry of Bax in H12299 and H1299-wt *p53* cells is illustrated in Figure 9B.

Discussion

Lung cancer has been identified as the most lethal form of cancer and is classified into two main types, small cell lung carcinoma (SCLC) and NSCLC, based on the invading cell

morphology. NSCLCs are more to be resistant to chemotherapy (28, 29). Therefore, demands for efficient therapy are needed to control growth and multiplication of this type of cancer.

One of the most important challenges in the development and the design of new anticancer agents is the understanding of the molecular differences between tumor and normal cells, which can help to target new anticancer agents to eliminate cancer cells with a reduced cytotoxic effect on normal cells. Our data showed two interesting analogs that were cytotoxic towards lung cancer cell lines but have less cytotoxic effect towards normal cells. Many drugs have been used for the treatment of lung cancer cells by inducing apoptosis through pathways that are *p53*-dependent and independent (3, 7, 30). *p53*, a tumor suppressor protein, is an essential mediator in the cellular response to DNA damage by causing G₁/G₂ cell cycle arrest and/or apoptosis (31). However, apoptosis susceptibility does not always correlate with *p53* expression and in many cases it is tissue- and cell-type specific (9-11). Compounds that could increase *p53* activity would be very beneficial to cancer therapy. On the other hand, over 50% of human tumors have mutations in *p53*, therefore agents that do not rely on *p53* activity are also appealing. In this work,

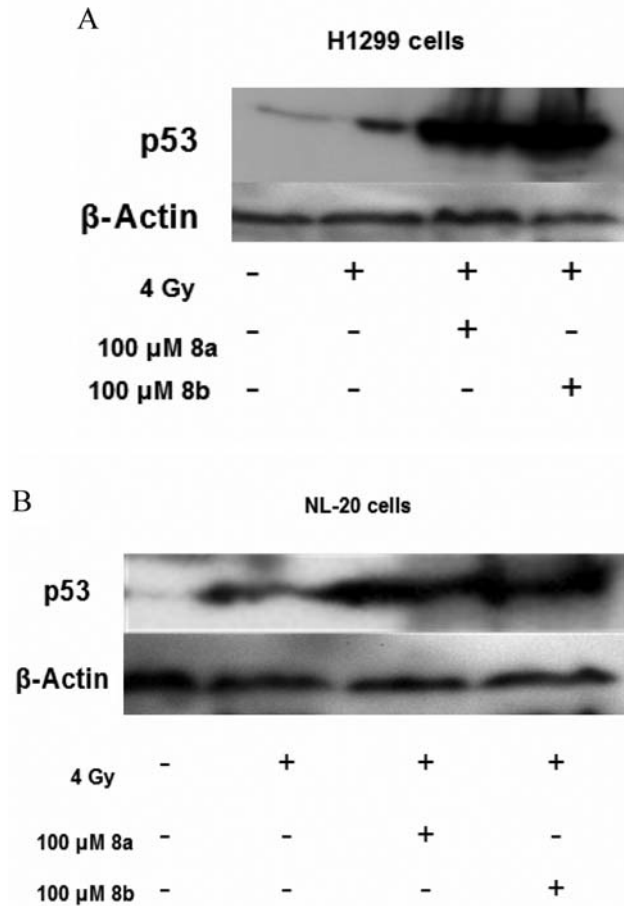


Figure 8. Western blot analysis. p53 expression was compared in stably transfected H1299 cells and NL-20 cells (B) in the presence of 100 μM 8a and 8b in combination with 4 Gy compared to irradiated group only and control groups. β-Actin was used as an internal control to monitor equal protein sample loading.

two interesting analogs, 8a and 8b, induced apoptosis in p53-independent mechanisms in H1299 cells and they also induced apoptosis to a lesser extent in H1299 cells stably transfected with p53. They have the least effect on NL-20 cells. The pharmacological bypassing of G₂ checkpoints is a powerful strategy for increasing the response to chemotherapy and radiotherapy (32, 33). Hence, combined treatment with cytotoxic agents is designed to circumvent the radiation-induced G₂ checkpoint, while at the same time maintaining the benefits of an intact G₁ checkpoint in normal cells (34, 35). The cell cycle checkpoints G₁ and G₂ were abrogated by quinuclidinone analogs in H1299 cells due to the absence of p53 function. In NL-20 cells and p53 stably transfected cells, p53 has more control on cell cycle checkpoints and fewer cells were directed to apoptosis. In this work, we report that 8a and 8b induced apoptosis *via* a decrease in the percentage of cells in the G₂/M phase. It also

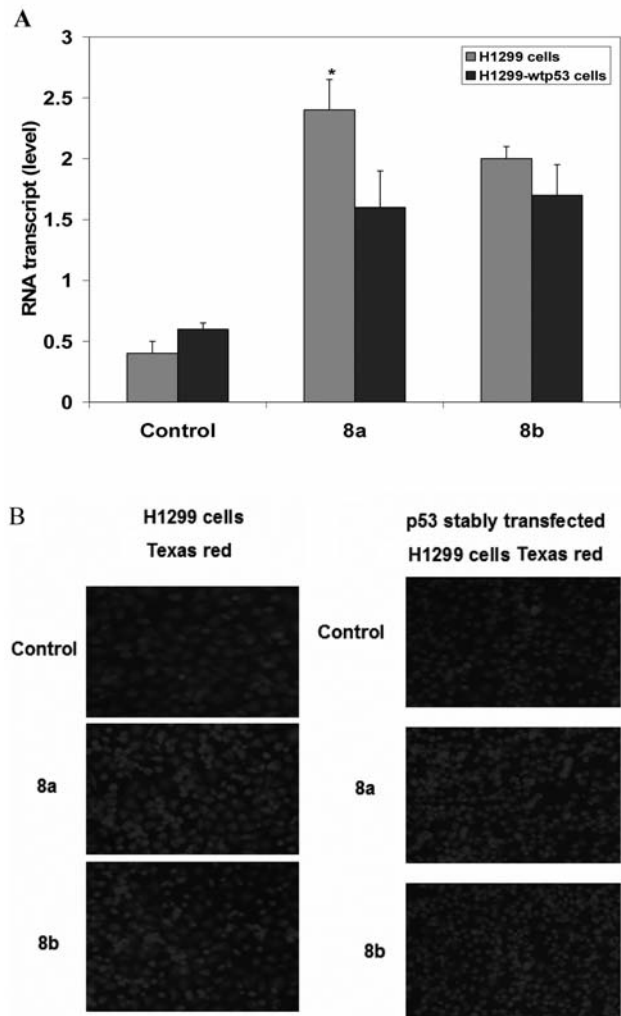


Figure 9. mRNA was extracted and was reverse transcribed to cDNA for real-time PCR analysis of mRNA level (A). Each data point is an average of three independent experiments and expressed as the mean ± SD. Immunohistochemistry of BAX in the presence and absence of 8a and 8b in H1299 and H1299-wt p53 (B).

increased the sensitivity of H1299 cells to radiation, as indicated by clonogenic survival assay, and a greater induction of apoptosis, as indicated by flow cytometric analysis data. Cyclin B1 has been classified as a G₂ cyclin because the accumulation of this protein begins at the S phase. It is essentially restricted to the G₂-M transition, reaches a maximal level at mitosis, and then is rapidly degraded at metaphase-anaphase transition. The protein complex of cyclin B1 and cyclin-dependent protein kinase 1 induces phosphorylation of key substrates that mediate cell cycle transition during the G₂-M phase (36). Our data indicated that 8a, which is a potent analog, increased cyclin B level in H1299 cells, while it did not have any significant effect in H1299-wt p53 cells.

Many different pathways may lead to the same chemotherapeutic-induced apoptosis, therefore, it becomes pertinent to identify the key players involved in the apoptotic process induced by quinuclidinone derivatives. Some death receptors, such as TNF- α , Fas and TRAIL, can activate SMase, causing the hydrolysis of sphingomyelin to diacylglycerol and ceramide. Ceramide is an important second messenger that carries the signal of apoptosis forward (37-39). The role of SMase activation and the subsequent release of ceramide was observed in some of the initial studies of doxorubin, cisplatin and gemitabine, but was activated in normal and cancer cells at similar levels (17, 18). Intriguingly, SMase activity in 8a-treated cells was more significantly affected in cancer cells more than normal cells. Caspase-3 plays a crucial role in DNA damage-induced apoptosis because it is frequently activated during apoptosis which is induced by various death stimuli, including anticancer drugs (26, 27). In the present study, we show that caspase-3 is required for IR- and 8a and 8b-induced apoptosis of H1299 cells with PARP-1 cleavage and *p53*-stably transfected cells though there was non-significant increase in caspase-3 activity in NL-20 cells. We found that SMase was stimulated in H1299 cells by the quinuclidinone analog 8b, with a concomitant increase in caspase-3 activity, as a key factor in the execution phase of apoptosis. Quinuclidinones 8b and 8c increased in NL-20 cells but did not induce apoptosis as in H1299 cells, perhaps due to a non-significant increase in caspase-3 activity.

COX-2 is overexpressed in many types of tumors, including lung cancer and of NSCLC in particular (40). It has been documented that there is a reduced risk of NSCLC with an increase use of aspirin, as it is a typical COX-2 inhibitor. There are many COX-2 inhibitors that have potential inhibitory effects on NSCLC (41-43). Moreover, Celecoxib had a cancer preventive effect and it reduced tumor growth in a number of tumor types such as NSCLC (44). Our novel derivatives showed a significant reduction of COX-2 activity in NSCLC with deletion of *p53*.

p53 is an attractive target for treatment with gamma radiation and other anticancer agents because of its important role in inducing apoptosis (9). However there are contradictory reports about the role of *p53* in chemosensitivity and radiosensitivity. Many studies reveal the role of wild-type *p53* in chemosensitivity, such as in breast carcinoma, colorectal carcinoma and soft tissue sarcoma, with chemotherapeutic agents such as doxorubicin, 5-FU and topotecan (10, 11). On the other hand, other groups report that inactivation of *p53* enhanced sensitivity to multiple anticancer drugs (5, 6). Thus, the role of *p53* and the use of various anticancer drugs, in combination with radiation, may well be tissue- and tumor-type specific. Both quinuclidinone analogs 8a and 8b increased expression of *p53* in NL-20 cells and *p53* stably transfected cells. BAX, a member of the BCL-2 family, plays key role in

mediating the apoptotic response. After DNA damaging signals, cytosolic BAX translocates to the mitochondria and homodimerizes, and then is thought to cause the release of cytochrome c which initiates the program of cell death (45). Our results showed that 8a and 8b significantly increases BAX expression in *p53* null cells more than *p53* stably transfected cells, indicating that BAX-induced apoptosis might receive signaling independent of *p53*. Here, we report potential novel anticancer drugs which induce cellular death of cancer cells *versus* normal cells, initiating a path for target based drug development. Investigational studies with more cancer cell lines and *in vivo* studies are in progress on these novel analogs.

Acknowledgements

This work has been supported by Science and Technology Development Fund, STDF, Cairo, Egypt.

References

- Herr I and Debatin KM: Cellular stress response and apoptosis in cancer therapy. *Blood* 98: 2603-2614, 2001.
- Kaufmann SH and Earnshaw WC: Induction of apoptosis by cancer chemotherapy. *Exp Cell Res* 256: 42-49, 2000.
- Malki A, Pulipaka A, Susan S and Bergmeier S: Structure activity studies of quinuclidinone analogs as antiproliferative agents in lung cancer cell lines. *Bioorg Med Chem Lett* 16: 1156-1159, 2006.
- Zhan Q, Carrier F and Fornace AJ: Induction of cellular *p53* activity by DNA-damaging agents and growth arrest. *Mol Cell Biol* 13: 4242-4250, 1993.
- Fan S, Smith ML and Rivet DJ: Disruption of *p53* function sensitizes breast cancer MCF-7 cells to cisplatin and pentoxifylline. *Cancer Res* 55: 1649-1654, 1995.
- Hawkins DS, Demers GW and Galloway DA: Inactivation of *p53* enhances sensitivity to multiple chemotherapeutic agents. *Cancer Res* 56: 892-898, 1996.
- Malki A and Susan S: Differential effect of selected methylxanthine derivatives on radiosensitization and cell cycle of normal and lung cancer cell lines. *Exp Oncol* 28(1): 18-24, 2006.
- Seth P, Katayose D, Li Z, Kim, M., Wersto R, Craig C, Shanmugam N, Ohri E, Mudahar B, Rakkar AN, Kodali P and Cowan K: A recombinant adenovirus expressing wild-type *p53* induces apoptosis in drug-resistant human breast cancer cells: a gene therapy approach for drug-resistant cancers. *Cancer Gene Ther* 4: 383-390, 1997.
- Steele RJ, Thompson AM, Hall PA and Lane DP: The *p53* tumour suppressor gene. *Br J Surg* 85: 1460-1467, 1998.
- Yang B, Eshleman JR, Berger NA and Markowitz SD: Wild-type *p53* protein potentiates cytotoxicity of therapeutic agents in human colon cancer cells. *Clinical Cancer Res* 2: 1649-1657, 1996.
- Zhan M, Yu D, Lang A, Li L and Pollock RE: Wild-type *p53* sensitizes soft tissue sarcoma cells to doxorubicin by down-regulating multidrug resistance-1 expression. *Cancer* 92: 1556-1566, 2001.
- Hanahan D and Weinberg RA: The hallmarks of cancer. *Cell* 100: 57-70, 2000.

- 13 Liscovitch M and Cantley LC: Lipid second messengers. *Cell* 77: 329-334, 1994.
- 14 Saddoughi SA, Song P and Ogretmen B: Roles of bioactive sphingolipids in cancer biology and therapeutics. *Subcell Biochem* 49: 413-440, 2008.
- 15 Smyth ML, Obeid LM and Hannun YA: Ceramide a novel lipid mediator of apoptosis. *Adv Pharmacol* 41: 133-154, 1997.
- 16 Sonnino S, Aureli M, Loberto N, Chigorno V and Prinetti A: Fine tuning of cell functions through remodeling of glycosphingolipids by plasma membrane-associated glycohydrolases. *FEBS Lett* 584: 1914-1922, 2010.
- 17 Lacour S, Hammann A, Grazide S, Lagadic-Gossmann D, Athias A, Sergent O, Laurent G, Gambert P, Solary E and Dimanche-Boitrel MT: Cisplatin-induced CD95 redistribution into membrane lipid rafts of HT29 human colon cancer cells. *Cancer Res* 64(10): 3593-3598, 2004.
- 18 Morita Y, Perez GI and Paris F: Oocyte apoptosis is suppressed by disruption of the acid sphingomyelinase gene or by sphingosine-1-phosphate therapy. *Nat Med* 6(10): 1109-1114, 2000.
- 19 Hwang D, Scollard D, Byrne J and Levine E: Expression of cyclooxygenase-1 and cyclooxygenase-2 in human breast cancer. *J Natl Cancer Inst* 90: 455-460, 1998.
- 20 van Rees BP, Saukkonen K and Ristimaki A: Cyclooxygenase-2 expression during carcinogenesis in the human stomach. *J Pathol* 196: 171-179, 2002.
- 21 Shirahama T and Sakakura C: Overexpression of cyclooxygenase-2 in squamous cell carcinoma of the urinary bladder. *Clin Cancer Res* 7: 558-561, 2001.
- 22 Soslow RA, Dannenberg AJ, Rush D, Woerner BM, Khan KN, Masferrer J and Koki AT: COX-2 is expressed in human pulmonary, colonic and mammary tumors. *Cancer* 89: 2537-2645, 2000.
- 23 Eberhat CE, Coffey RJ, Radhika A, Giardiello FM, Ferrenbach S and DuBois RN: Up-regulation of cyclooxygenase-2 gene expression in human colorectal adenomas and adenocarcinomas. *Gastroenterology* 107: 1183-1188, 1994.
- 24 Reddy BS, Hirose Y and Lubet R: Chemoprevention of colon cancer by specific cyclooxygenase-2 inhibitor, celecoxib, administered during different stages of carcinogenesis. *Cancer Res* 60: 293-297, 2000.
- 25 Ziegler J: Early trials probe COX-2 inhibitors' cancer-fighting potential. *J Natl Cancer Inst* 91: 1186-1187, 1999.
- 26 Oliver L and Vallette FM: The role of caspases in cell death and differentiation. *Drug Resist Updat* 8(3): 163-170, 2005.
- 27 Fischer U, Janicke RU and Schulze-Osthoff K: Many cuts to ruin: a comprehensive update of caspase substrates. *Cell Death Differ* 10(1):76-100, 2003.
- 28 Alberg AJ and Samet JM: Epidemiology of lung cancer. *Chest J* 123(1 Suppl): 21S-49S, 2003.
- 29 Schwartz AG: genetic predisposition to lung cancer. *Chest* 125(5 Suppl): 86S-89S, 2004.
- 30 Adachi H, Preston G, Harvat B, Dawson MI and Jetten AM: Inhibition of cell proliferation and induction of apoptosis by the retinoid AHPN in human lung carcinoma cells. *Am J Respir Cell Mol Biol* 18(3): 323-233, 1998.
- 31 Di Leonardo A, Linke S, Clarkin K and Wahl G: DNA damage triggers a prolonged p53-dependent G₁ arrest and long-term induction of *Cipl* in normal human fibroblasts. *Genes Dev* 8(21): 2540-2551, 1994.
- 32 Tenzer A and Pruschy M: Potentiation of DNA-damage-induced cytotoxicity by G₂ checkpoint abrogators. *Current Med Chem* 3: 35-46, 2003.
- 33 Yu Q, La Rose J, Zhang H, Takemura H, Kohn KW and Pommier Y: UCN-01 inhibits p53 up-regulation and abrogates gamma-radiation-induced G(2)-M checkpoint independently of p53 by targeting both of the checkpoint kinases, Chk2 and Chk1. *Cancer Res* 62: 5743-5748, 2002.
- 34 Aldridge DR and Radford IR: Explaining differences in sensitivity to killing by ionizing radiation between human lymphoid cell lines. *Cancer Res* 58: 2817-2824, 1998.
- 35 Bunch RT and Eastman A: Enhancement of cisplatin-induced cytotoxicity by 7-hydroxystaurosporine (UCN-01), a new G₂-checkpoint inhibitor. *Clin Cancer Res* 2: 791-797, 1996.
- 36 Nobury C and Nurse P: Animal cell cycles and their control. *Trends Biochem Sci* 19: 143-145, 1992.
- 37 Gulbins E, Bissonnette R, Mahboubi A, Martin S, Nishioka W, Brunner T, Baier G, Baier-Bitterlich G, Byrd C and Lang F: FAS-induced apoptosis is mediated via a ceramide-initiated RAS signaling pathway. *Immunity* 2(4): 341-351, 1995.
- 38 Hannun YA and Obeid LM: Ceramide: an intracellular signal for apoptosis. *Trends Biochem Sci* 20(2):73-77, 1995.
- 39 Jarvis WD, Kolesnick RN, Fornari FA, Traylor RS, Gewirtz DA and Grant S: Induction of apoptotic DNA damage and cell death by activation of the sphingomyelin pathway. *Proc Natl Acad Sci USA* 91(1): 73-77, 1994.
- 40 Sandler AB and Dubinett SM: COX-2 inhibition and lung cancer. *Semin Oncol* 31(2): 45-52, 2004.
- 41 Huang M, Sharma S, Mao JT and Dubinett SM: Non-small cell lung cancer-derived soluble mediators and prostaglandin E₂ enhance peripheral blood lymphocyte IL-10 transcription and protein production. *J Immunol* 157: 5512-5520, 1996.
- 42 Wolff H, Saukkonen K, Anttila S, Karjalainen A, Vainio H and Ristimaki A: Expression of cyclooxygenase-2 in human lung carcinoma. *Cancer Res* 58: 4997-5001, 1998.
- 43 Pöld M, Zhu LX, Sharma S, Burdek, M, Lin Y, Pold A, Krysan A, Moa J, Batra R, Strieter, R and Dubinett S: Cyclooxygenase-2-dependent expression of angiogenic CXC chemokines, ENA-78/CXCL5 and IL-8/CXCL8, in human non-small cell lung cancer. *Cancer Res* 64: 1853-1860, 2004.
- 44 Howe LR, Subbaramaiah K, Patel J, Masferrer KL, Deora A, Hudis C, Thaler HT, Muller W, Du, Brown A and Dannenberg AJ: Celecoxib, a selective cyclooxygenase 2 inhibitor, protects against human epidermal growth factor receptor 2 (HER-2)/neu-induced breast cancer. *Cancer Res* 62: 5405-5417, 2002.
- 45 Cory S and Adams JM: The Bcl2 family: regulators of the cellular life or death switch. *Nat Rev Cancer* 2: 647-656, 2002.

Received February 15, 2011

Revised March 19, 2011

Accepted March 21, 2011